Analysis of Shoreline Changes for the Western Tombolo of Giens

V.V. Than [a,b*], Y. Lacroix [c,d]
[a] Faculty of Civil Engineering, Thuyloi University (TLU), Tay Son street, Dong Da, Ha Noi, Viet Nam
[b] I2M, AMU, 39 rue F. Joliot Curie, 13453 Marseille Cedex 13, France
[c] SEATECH, avenue G. Pompidou, 83162 La Valette du Var, France
[d] MEMOCS, Università Degli Studi dell'Aquila, Palazzo Caetani, 04012 Cisterna di Latina, Italy

ABSTRACT
The Western tombolo of Giens in the South of France is submitted to shoreline retreats and coastal erosion. We use statistical techniques in order to better understand an overall trend of the shoreline erosion. Our aim is to evaluate the historical and future shoreline changes. All available data about shoreline concerning the site from 1920 to 2012 were gathered. The statistical methods from Digital Shoreline Analysis System are used to estimate the overall change in shoreline position and shoreline change rates. The results demonstrate a clear shoreline dynamics and annual shoreline change rates for four sectors of the Western tombolo. The trends of shoreline changes, the relationship between shoreline changes and some factors of coastal erosion (wave, sea level rise, beach slope, and shoreline orientation) in the Western tombolo of Giens are discussed. We estimate that the average annual rate of shoreline erosion is (-0.01 to -0.63) ± (0.27 to 1.82) meters per year in the northern part and the shoreline accretion is (0.02 to 2.01) ± (0.14 to 5.10) meters per year in the central and southern part of the Western tombolo. Individual rates along some transects in northern part of the Western tombolo reach as high as -1.17 ± 0.5 meters per year.

Keywords: Shoreline retreat, wave, sea level rise, beach slope, shoreline orientation, DSAS.

1. Introduction
The double tombolo of Giens is between the Gulf of Giens and Hyères harbor, located in the Hyères Township in the Var department, France. This tombolo is formed from two sand dunes: western and eastern arrows. The Almanarre beach is located at the western branch. It has a total extent of 4 km of straight sandy beach, along the Salt Road (Fig. 1).
Since the 50s, there have been many studies about the tombolo to discover the causes of the erosion and evaluate the coastal erosion (Lacroix et al. 2015a). However, the coastal erosion process is still not well understood.
Worldwide, 70% of beaches tend to recede while only 10% fatten. The shoreline retreats affect many countries in Europe. Actually, about 20% of coasts are affected by shoreline erosion (Than 2015).
The majority of French beaches are concerned by the phenomenon of erosion. A quarter of the metropolitan coast (24.2%), or 1723 km of coastline, retreats under the action of the sea. In contrast, 43.7% of the coastline representing a linear distance of 3115 km are stable and almost 10% of the coastline are expanding and gain lands from the sea (IFEN 2007). On the French Mediterranean coast, 50% of beaches tend to erode, the Languedoc beaches are the most affected, 76 km of the Languedoc-Roussillon coastline is suffering uncontrolled erosion over a total of 356 km of coastline. The coastal erosion phenomenon in Saintes-Maries-de-la-Mer, Camargue, causes the coastline to retreat ranging from 2.5 and up to 12 m/yr locally.
The Provence-Alpes-Côte d'Azur (PACA) coastlines are no exception to this evolution. The maximal erosion rate estimated by GEOMER (1996) for the period from 1954 to 1993 is -1.5 m/yr from the mouth of the Gapeau river to approximately 800 m south (in the town of Hyères, PACA) (Courtaud 2000). Individual shoreline erosion at Cabanes du Gapeau reaches as high as -40 m between 1969 and 1975 (Courtaud 2000). For the Western tombolo, the average shoreline retreat estimate for 3000 years is -0,1 m/yr (Courtaud 2000).

[*] *Corresponding author at: Faculty of Civil Engineering, Thuyloi University (TLU), street Tay Son, Dong Da, Ha Noi, Viet Nam. Tel.: +84919685246.*
E-mail addresses: thanvanvan@tlu.edu.vn (V.V. Than)

The shoreline change analysis is of primary interest from the coastal manager's areas (Dang and Pham 2008). The shoreline evolution can be often divided into three overall categories: eroding, equilibrium, and accreting (Salghuna and Bharathvaj 2015).

The focus on our work is the application of Digital Shoreline Analysis System (DSAS) to analyze shoreline movements, identify the erosional and accretional trends, with different timescales (long, medium, and short term) based on the 1920 to 2012 coastlines. We also predict future trends of shoreline movements. This study determines the regressions between shoreline change and some agents of coastal erosion (wave, sea level rise, beach slope, and shoreline orientation) in the Western tombolo of Giens.

1.1. Geomorphological Conditions

The coastline of the Western tombolo has been classified into four sectors that correspond to the four hydro-sedimentary cells (Lacroix et al. 2015b), based on the geo-morphology and their limiting landmarks (Fig. 1).

Table 1 represents the geometries of the coastline of the Western tombolo (Lacroix et al. 2015b).

Table 1

Coastline of the Western tombolo of Giens (Lacroix et al. 2015b).

Sector	Zone	Limiting landmarks	Length (m)
1	North	northern end of the shoreline, B01 to B03	1 125
2	North-central	B03 to B16	1 275
3	Central	B16 to B23	675
4	South	B23 to B46, southern end of the shoreline	2 975
Total			6 050

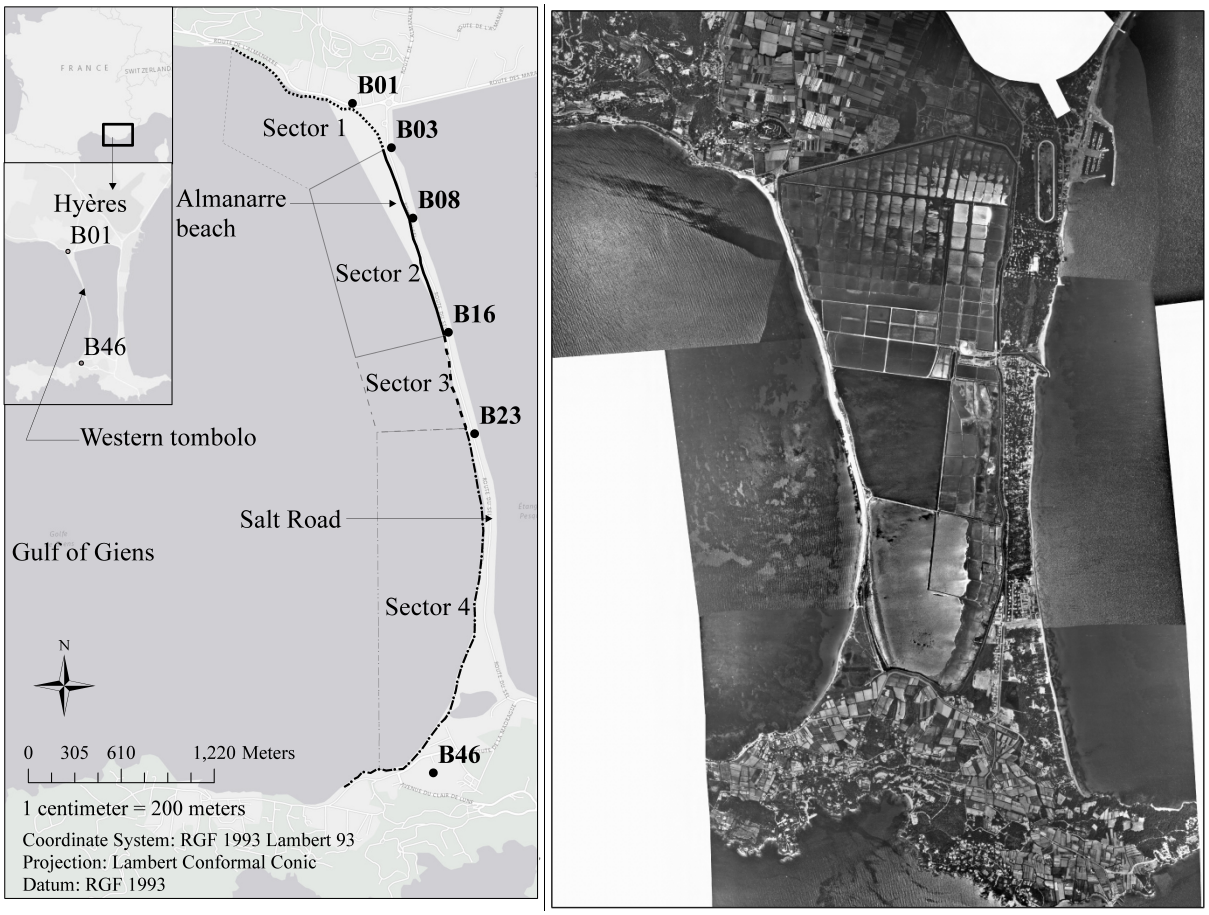

Fig. 1. (A) Location of the Almanarre beach and Salt Road along the Western tombolo of Giens and four sectors 1-4 from north to south of the coastline of the Western tombolo. (B) Aerial photographs for tombolo of Giens in 1971.

The sector 1 of the coastline of the Western tombolo, which is about 1.1 km, stretches from the extreme northern end of the shoreline which includes landmarks B01 to B03. Then, the sector 2 covers about 1.3 km of the coastline of the Western tombolo, from the landmark B03 to B16. The coast of the Central Zone is about 0.7 km, from B16 to B23. The shoreline of the South Zone is the longest, about 3 km.

A mean slope was estimated from 0.9 to 1% for the area of study. A distance from the coast to the 30 m isobaths was reported at 3.2 km (Lacroix et al. 2015a).

1.2. Wind Conditions

Two prevailing wind regimes were identified (Blanc 1974; Farnole et al. 2002; IARE 1996; Jeudy De Grissac 1975). The western regime represents 70% of the total, which generates a stir in the Gulf of Giens. Eastern regime represents 30% of the total and has no influence on the study area which is protected by the tombolo and the peninsula.

1.3. Hydrodynamic Conditions

The water level data are available at Toulon station. The data recorded in Toulon are discontinuous (a few years and often incomplete). However, changes in the sea level of tombolo are regularly described using data from Toulon station (Courtaud 2000; IARE 1996; SOGREAH 1988b). The tides in the study area do not exceed 0.3 m.

The wave is characterized by strong seasonality: actually, increased wave's amplitude happens in the early fall, in winter, and during the spring equinox storms; the amplitudes of the wave have the lowest values in summer. The highest amplitude of the offshore wave is at least greater than 1.25 m, corresponding to the three dominant directions, North-West, South-West, and East (Courtaud 2000). Western and South-Western agitations with medium near-shore wave's amplitude are predominant (HYDRO M 1993). The near-shore wave's amplitude may vary depending on the presence of Posidonia and sandstone outcrops (Luhar et al. 2010). The dominant near-shore waves are South-South-West to South-West in the Gulf of Giens (Lacroix et al. 2015a).

At 4 m isobaths in northern part of Almanarre beach, the average current speed is between 3 and 7 cm/s in calm conditions and increases 15 to 25 cm/s in storm conditions (Lacroix et al. 2015a). The dominant directions on average are East to South and West to North (Lacroix et al. 2015a).

1.4. Geomorphologic and Biologic Ground Conditions

The geology of the area generally comprises rock, gravels and fine sand (Blanc 1960; SOGREAH 1988a). In the Gulf of Giens, the Posidonia meadows reduce wave energy and protect the Almanarre beach from coastal erosion.

2. Materials and Methods

First, the shoreline change analysis method will be presented. Then, the shoreline positions will be collected.

2.1. Workflow Methodology

In this study, two techniques were used: shoreline extraction techniques and shoreline change analysis techniques. Fig. 2 shows a workflow methodology:

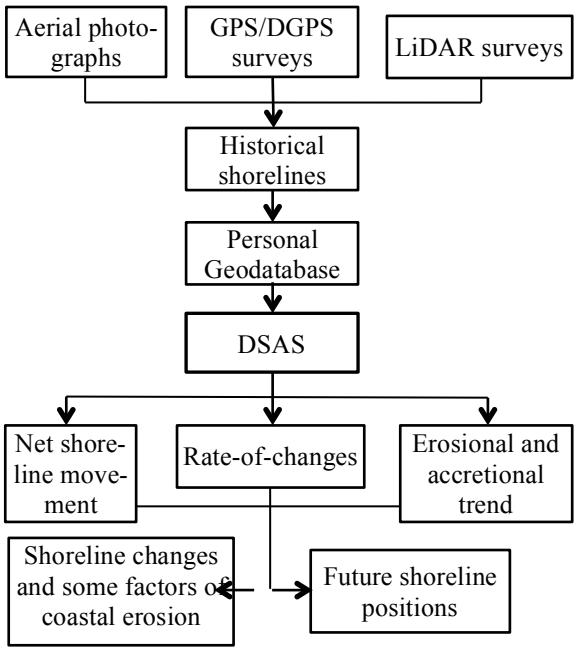

Fig. 2. Methodology for the shoreline change analysis.

First, the shoreline extraction techniques were mentioned in many studies. The techniques used in our work are based on photo-interpretation techniques, developed by CEREGE and Courtaud (2000), and shoreline extraction techniques from GPS, DGPS and LiDAR surveys (Fig. 2).
Second, the DSAS tool was applied to analyze shoreline change (Fig. 2). The overall change in shoreline position (in meters) was investigated by using Net Shoreline Movement (NSM) method (Fig. 2). The annual shoreline change rates (in meters per year) is estimated at each transect by three statistical methods: End Point Rate (EPR), Weighted Linear Regression (WLR), and Linear Regression Rate (LRR). The short, medium, and long term shoreline change rates are estimated for this study.
Third, an extrapolation of the average annual shoreline change rates was used to predict future shoreline movements (Fig. 2).
Finally, the regressions of the shoreline changes and some agents of coastal erosion (wave, sea level rise, beach slope, and shoreline orientation) were analyzed (Fig. 2).

2.2. Shoreline Positions Acquisition

In this study, some sources were used to define the shoreline positions. The coastlines data used for our work are acquired from CEREGE (Centre de Recherche et d'Enseignement de Géosciences de l'Environnement) association and Courtaud (2000) from 1920 to 1998. Table 2 reviews the aerial photographs for tombolo of Giens (Fig. 1B) from the public and private organisms (Courtaud 2000). The shoreline positions were extracted from aerial photographs by some organisms, namely IGN, Centre Camille Jullian (CNRS, Aix-en-Provence), Société Aérial (Aix-Les Milles) (Table 2). This database includes twelve shorelines of 1920, 1950, 1955, 1960, 1970, 1971, 1984, 1987, 1991, 1994, 1995, and 1998. The different steps of data processing of these aerial photographs are described by Courtaud (2000): selection of a reference picture, geometric rectification of the aerial photographs available, and finally digitization of the coastline and error estimate.

The 2000 to 2010 and 2012 coastlines were extracted from GPS, DGPS and LiDAR surveys (bathymetry and topography data) from EOL (Étude et Observation du Littoral) and SHOM (Service Hydrographique et Océanographique de la Marine) association, respectively.

Table 2

Aerial photographs for tombolo of Giens from the public and private organisms (Courtaud 2000).

Year	Organism	Year	Organism	Year	Organism	Year	Organism
1940 to 1944	Centre Camille Jullian	1972	IFN	1982	IGN	1991	IGN
1950	IGN	1976	IGN	1984	Société Aérial	1993	IGN
1955	IGN	1977	IGN	1987	IGN	1994	Société Aérial
1960	IGN	1978	IGN	1988	IGN	1997	IGN
1971	IGN	1979	IGN	1989	IGN	1998	IGN

All shoreline data were projected to the same geographical system (Lambert 93) (Faye et al. 2011). A shoreline data is a shapefile (format *.shp). The shoreline must have date, length, ID, shape, and uncertainty attributes. The date's historical shoreline position was added for the date attribute under format MM/DD/YYYY.

The shoreline uncertainty was calculated and entered for the uncertainty attribute. The other attributes (length, ID and shape) were automatically generated in Arcgis 10, once a shapefile was created. Finally, a collection of shoreline positions was obtained under shapefile format for the entire period 1920-2012 including twenty-four shoreline positions for 1920, 1950, 1955, 1960, 1970, 1971, 1984, 1987, 1991, 1994, 1995, 1998, 2000-2010, and 2012.

2.3. Data Uncertainty

The analysis of data uncertainty will depend on the collected data's source for periods 1920 to 1998 and 2000 to 2012.

2.3.1. Data for period 1920 to 1998

First, the types of uncertainty will be described. Then, the total positional uncertainty will be estimated.

2.3.1.1. Types of Uncertainty

There are two types of uncertainty: positional uncertainty and measurement uncertainty (Fletcher et al. 2011). Five main sources of error were evaluated in detecting shoreline positions from the aerial photographs used for this study, namely seasonal error, tidal fluctuation error, digitizing error, pixel error and rectification error (Fletcher et al. 2011; Romine and Fletcher 2012).

a. Positional Uncertainties

They are errors related to seasons and tides (Fletcher et al. 2011).

• Seasonal error (E_s)

It is the error from movements in shoreline position (seasonal shoreline fluctuations) under the action of the waves and storms (Fletcher et al. 2011).

Seasonal shoreline position differences were calculated on the spring and fall beach profiles from the EOL measurements at the Almanarre beach (Fig. 3) (Fletcher et al. 2011).

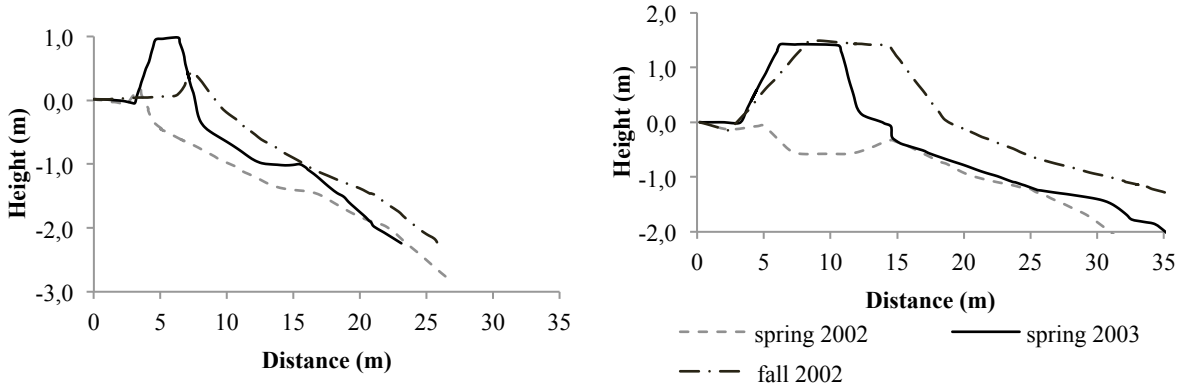

Fig. 3. Seasonal beach profile at the landmark B08 (left) and B11 (right) of the Western tombolo observed at different seasons from 2002 to 2003 (Serantoni and Lizaud 2000-2010).

The different steps of calculation of this error are described by Fletcher et al. (2011). Finally, the seasonal error was established ± 5 m.

• Tidal fluctuation error (E_t)

It is the error associated with horizontal variability in shoreline position due to tides (Fletcher et al. 2011). The tidal range (0.3 m) of the study area was unsignificant. The tidal fluctuation error thus is approximately 0 m (Addo et al. 2011).

b. Measurement Uncertainties

They are related to shoreline digitization, image resolution, and image rectification.

• Digitizing error (E_d)

It is the error related to shoreline digitization (Fletcher et al. 2011). The digitizing error was estimated about ± 4.5 m (Romine and Fletcher 2012).

• Pixel error (E_p)

It relates to image precision (resolution). It is the image pixel size (Fletcher et al. 2011). The image pixel size is from 2.5 to 5 m (Courtaud 2000). The graphic restitution of the coastline reveals a maximum deviation of ± 2 pixels (± 5-10 m) (Courtaud 2000). Thus, we suggest that average pixel error should be ± 7.5 m.

• Rectification error (E_r)

It is the square root of the mean error of the image rectification process (Fletcher et al. 2011; Romine and Fletcher 2012). The rectification error is proposed ± 0.1-7.3 m) (Romine and Fletcher 2012). We have decided that the rectification error may be ± 1 m (Robichaud et al. 2012).

2.3.1.2. Total Positional Uncertainty

The total positional uncertainty (U_t) is the result of all errors that were previously estimated. It is defined as the square root of the sum of the squares of the sources of previous errors (Fletcher et al. 2011; Romine and Fletcher 2012). It was calculated by using (1):

$$U_t = \pm \sqrt{E_s^2 + E_t^2 + E_d^2 + E_p^2 + E_r^2} \quad (1)$$

where E_s is the seasonal error, E_t is the tidal error, E_d is the digitizing error, E_p is the pixel error, and E_r is the rectification error.

The total positional uncertainties were used as weights (weighted linear regression or weighted least squares) in the shoreline change analysis in the DSAS.

The estimation of each type of error is enumerated in Table 3.

Table 3

Uncertainties for historical position shorelines for period 1920 to 1998.

Uncertainty	Positional uncertainty		Measurement uncertainty			Total positional uncertainty U_t (m)
	E_s (m)	E_t (m)	E_d (m)	E_p (m)	E_r (m)	
Value	± 5	≈ 0	± 4.5	± 7.5	± 1	± 10

The annualized uncertainty (U_a) is the uncertainty in the rate-determining model (error for the shoreline change rate) (Addo et al. 2011; Fletcher et al. 2011). As the shoreline change rate, it is expressed in m/yr. It was calculated as the square root of the sum of the squares of total positional uncertainty for each shoreline divided by the analysis period, as in (2) (Fletcher et al. 2011)

$$U_a = \pm \frac{\sqrt{\sum_1^n U_{ti}^2}}{T} \qquad (2)$$

where i is index of the shoreline, U_{ti} is the total positional uncertainty for each shoreline I, and T is the period of analysis.

2.3.2. Data for period 2000 to 2012

The mapping uncertainty is estimated as ± 5 m for the period from 2000 to the present (Anders and Byrnes 1991; Crowell et al. 1991; Moore 2000; Thieler and Danforth 1994). Thus, we suggest that an overall uncertainty should be ± 5 m for 2000 to 2012 shorelines.

2.4. Presentation of DSAS

DSAS version 4.3 tool developed by the USGS is an extension for ArcGIS version 10 software. It uses several statistical techniques to compare shoreline positions through time and evaluate shoreline changes.

There are many statistical approaches for the estimation of shoreline changes (Dang and Pham 2008; Jamont 2014), each method has advantages and drawbacks (Dang and Pham 2008; Genz et al. 2007; Thieler et al. 2003). The methods used in DSAS are described below. More details about other statistical parameters are described by Himmelstoss (2009).

2.4.1. Net Shoreline Movement (NSM)

NSM is associated with the dates of two shorelines. It reports a distance in meters. It calculates the distance between the oldest and the youngest shorelines at each transect (Oyedotun 2014). The overall change in shoreline position was investigated by using NSM (Oyedotun 2014).

2.4.2. Shoreline Change Envelope (SCE)

SCE calculates a distance in meters between "*the shoreline farthest from and closest to the baseline at each transect*" (Himmelstoss 2009). It is not associated with the dates of these shorelines (Himmelstoss 2009).

2.4.3. End Point Rate (EPR)

EPR is determined by dividing NSM by the time period elapsed, as in (3) (Chand and Acharya 2010; Faye et al. 2011; Himmelstoss 2009; Jamont 2014; Oyedotun 2014; Prukpitikul et al. 2012)

$$R = D/T_e \qquad (3)$$

where R is in meters per year (m/yr), D is in meters and T_e is the time period elapsed between the oldest and the most recent shoreline (years).

EPR still works well when we have only two shorelines to analyze the evolution (Thieler et al. 2005).

2.4.4. Linear Regression Rate (LRR)

LRR corresponds to the value of the slope of a least squares regression line, as in (4), that fits all points of intersection between all shorelines and a specific transect (Faye et al. 2011; Oyedotun 2014; Prukpitikul et al. 2012).

$$y = m.x + b \quad (4)$$

where y is the distance from baseline, m is the slope (LRR method), and b is y-intersect (where the line crosses the y-axis) (Himmelstoss 2009).

2.4.5. Weighted Linear Regression rate (WLR)

The WLR method uses a linear regression taking into account a weight (for each shoreline position) according to the shoreline uncertainty to determine a best-fit regression line. The weight is the inverse of the squared total positional uncertainty (Fletcher et al. 2011).

This method increases the influence of shoreline points with smaller total positional uncertainty on the best-fit regression line (Himmelstoss 2009). The slope of this regression line is the shoreline change rate in m/yr, as in (5).

$$y = m_w.x + b_w \quad (5)$$

where m_w is the slope (WLR method) and b_w is y-intersect (Himmelstoss 2009).

WLR method requires at least three historical shoreline positions (Fletcher et al. 2011).

2.4.6. Least Median of Squares (LMS)

LMS uses a weighted least-squares regression. The shoreline points with larger offsets (residuals) have less influence on the best-fit regression line (Himmelstoss 2009). The slope of this regression line is the value of LMS.

2.4.7. Standard Error of the Slope (LCI, WCI)

The standard errors of the slope with confidence interval LCI and WCI correspond to linear regression and weighted linear regression methods, respectively. It describes the uncertainties of the rate-of-change, in meters per year (Himmelstoss 2009).

2.4.8. Coefficient of Determination (R^2)

It *"is the percentage of variance in the data that is explained by a regression"* (Himmelstoss 2009). It is used to verify the quality of the best-fit line regression.

2.5. Determining the Period of Calculation

The period of calculation was divided into a long-term period and short and medium term periods.

2.5.1. Long-term period

The period of calculation of the shoreline change is 92 years from 1920 to 2012 (Than 2015). All shorelines were used to calculate in the DSAS for long-term period.

2.5.2. Short- to medium-term

To evaluate human impacts on the Almanarre beach, the shoreline data are divided into four groups that correspond to the short and medium term periods based on the human impacts:

- From 1920 to 1960: without human impact;
- From 1960 to 1971: installation of gabions, construction of the Salt Road;
- From 1971 to 1998: the establishment of wooden palisades, riprap revetment, "ganivelles", etc;
- From 1998 to 2012: the complete removal of riprap revetment, annual reconstitution of the sand dune.

The time intervals of each period vary from 11 to 40 years. It is enough to estimate the shoreline changes in the study area.

2.6. Configuration of DSAS

There are four main steps to configure DSAS:

For the first step, a baseline was defined in a shapefile format (*.shp) with many attributes (name, type, geographic properties). A baseline was created from north to south almost parallel to general orientation of the shoreline, through the landmarks B01-46 of EDF (Électricité de France). The baseline location is onshore. This baseline is used to calculate the distance from a shoreline to it at each orthogonal transect.

In a second step, a collection of shorelines and baselines was created in ArcGIS 10 for DSAS (Fig. 4A). A Personal Geodatabase (*.mdb) was created by using ArcCatalog in ArcGIS 10 for each period. The Feature Class (type of Line Features) of the shoreline and base line were created in each Personal Geodatabase. All shoreline positions for each selected period were appended to a single shapefile.

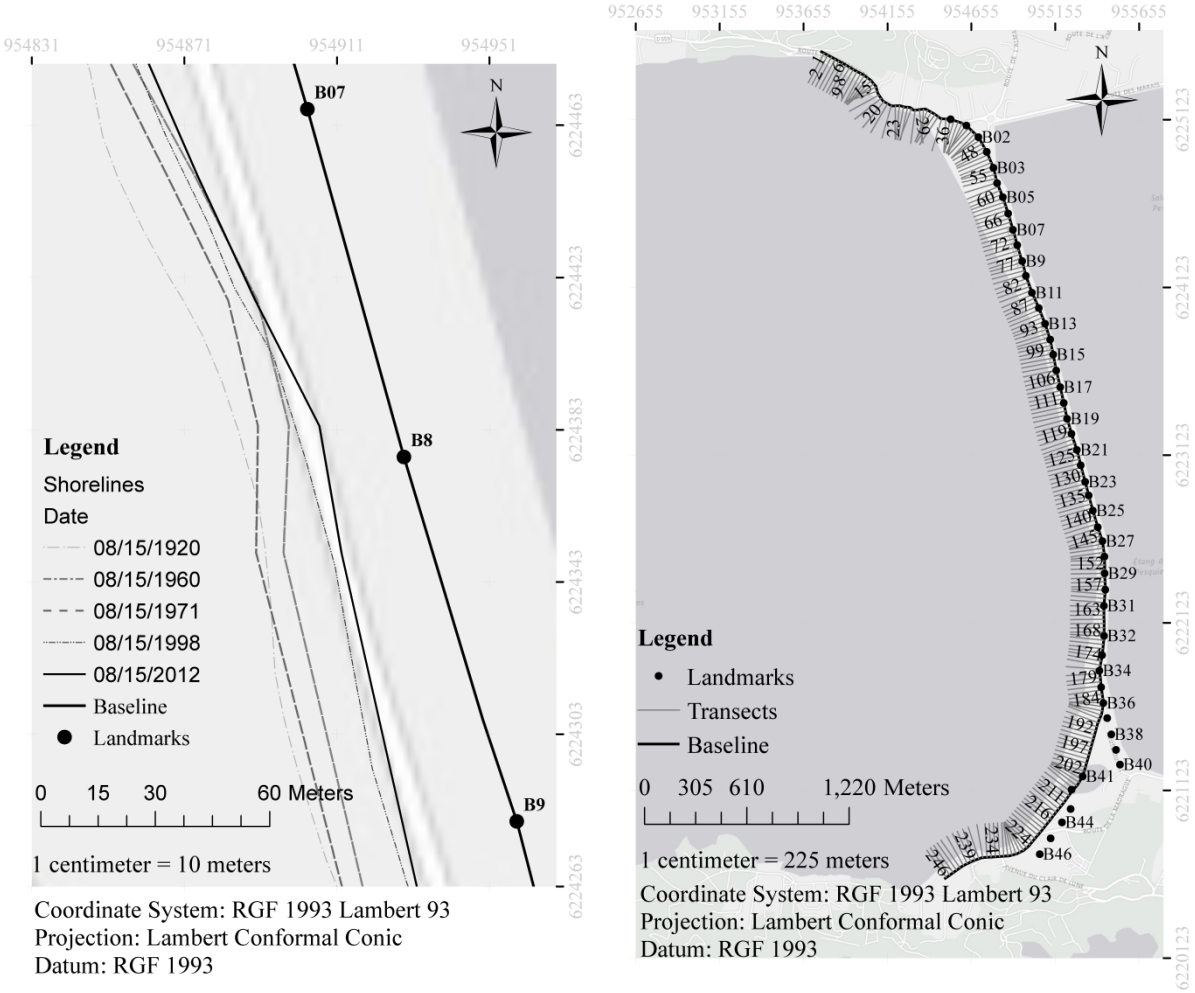

Fig. 4. (A) The shoreline positions observed at different years (1920-2012). (B) Transects created along the baseline and relative position of transects on system landmarks.

In a third step, the orthogonal transects were generated at a specified spacing alongshore by using DSAS, once the Personnal Geodatabase was ready in ArcGIS. They are equidistant perpendicular lines to the baseline. A total of 246 orthogonal transects was cast along the baseline from north to south at a 25 m spacing alongshore. The length of transect is 200 m. These transects span the entire coast from sector 1 to 4. They are numbered with Transects ID ordered from north (Transect ID 1) to south (Transect ID 246) (Fig. 4B). Transects that do not intersect at least three shorelines, are not included in the shoreline change analysis.

In the final step, after the creation of the orthogonal transects, DSAS calculates the overall change in shoreline position (distance of shoreline movement) by using NSM method. The rates of shoreline change along each transect were calculated for each period of calculation by using EPR, WLR, and LRR method. The regional change rate is calculated by averaging the rates of changes from all

transects in each studied sector. The coefficient of determination (R^2) is calculated by DSAS. The average coefficient of determination is the mean of these values at all transects. The uncertainties of the annual rate-of-change (m/yr) are the 95 percent confidence interval (LCI95 or WCI95).

3. Results

First, the Net Shoreline Movement is exposed. Then, the annual shoreline change rates are examined.

3.1. Net Shoreline Movement

The results are presented for each sector from 1 to 4:

3.1.1. Sector 1

Sector 1 is composed of 53 transects. It comes under transects number 1 to 53. Fig. 5 shows that the sector 1 includes a stable area between transects number 1 and 33. The South of sector 1 from transects number 33 to 46 that corresponds to the landmarks B01-B03 has positive shoreline movements before 1971. The negative shoreline movements are observed here after 1971 perhaps due to the existence of the Salt Road, riprap revetment, and Ceinture Canal, which influence on the natural sediment balance (Fig. 5).

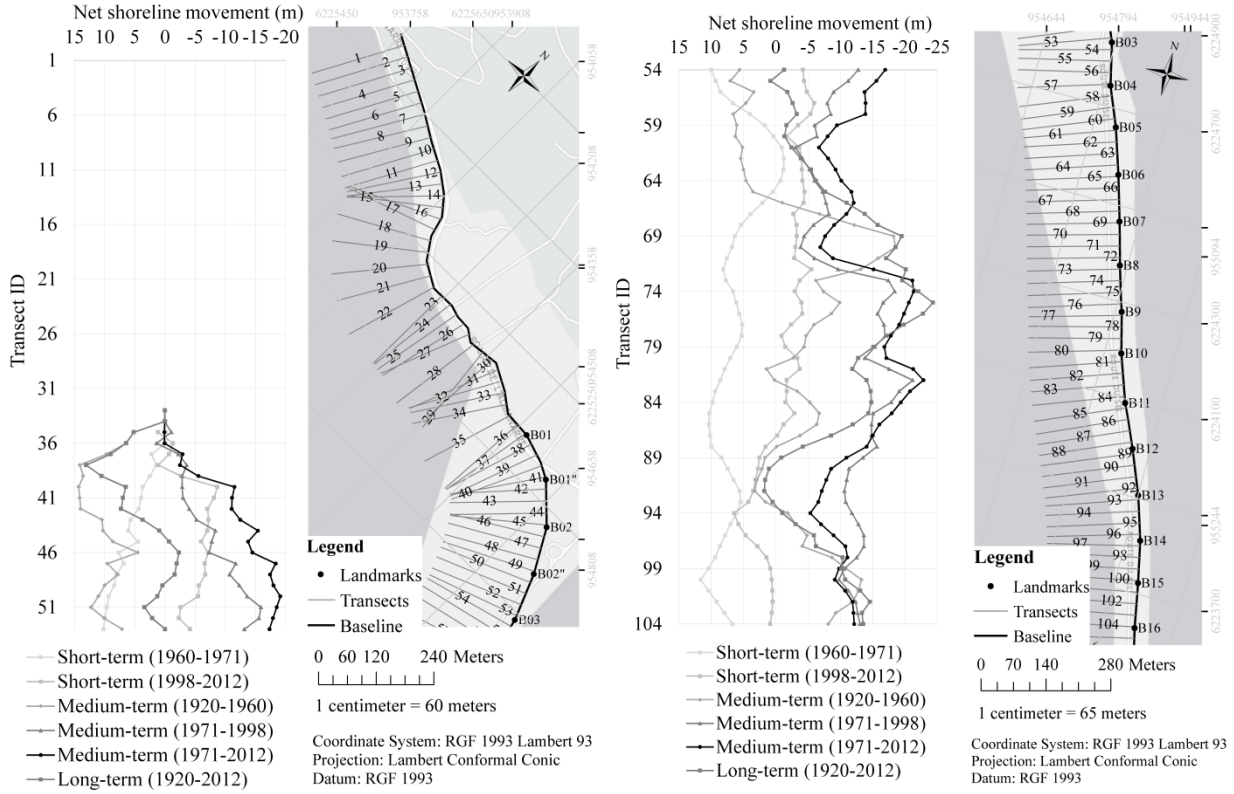

Fig. 5. Short, medium, and long term net shoreline movement along transects in the sectors 1 (left) and 2 (right) of the Western tombolo of Giens.

3.1.2. Sector 2

There are 51 transects for sector 2 (Fig. 5), from number 54 to 104.

Sector 2 has a positive value indicating accretion (maximum 12 m of NSM method) for short-term approach of 1960-1971 perhaps due to the existence of beach nourishment during the construction of the Salt Road (Fig. 5).

There are small accretion areas in the medium and short term periods of 1920-1960, 1998-2012 and long-term (1920-2012) at the northern and southern parts of this sector (Fig. 5).
Except two cases with accretion, we observe that this is a zone of erosion. Sector 2 has a negative value indicating erosion regarding medium-term approach of 1971-1998 due to the human impacts (Salt Road, riprap revetment, and Ceinture Canal) (Fig. 5).

3.1.3. Sector 3

Sector 3 is composed of 27 transects, number 105 to 131. We observe that the NSM for sector 3 regarding short-term period of 1998-2012 and long-term of 1920-2012 are opposite. Since 1971, this sector tends to be deposited because it is not as exposed as sector 2 to the south-western regime. We observe that transect number 117 near landmark B19 is stable for the periods of 1971-1998 and 1998-2012 (Fig. 6).

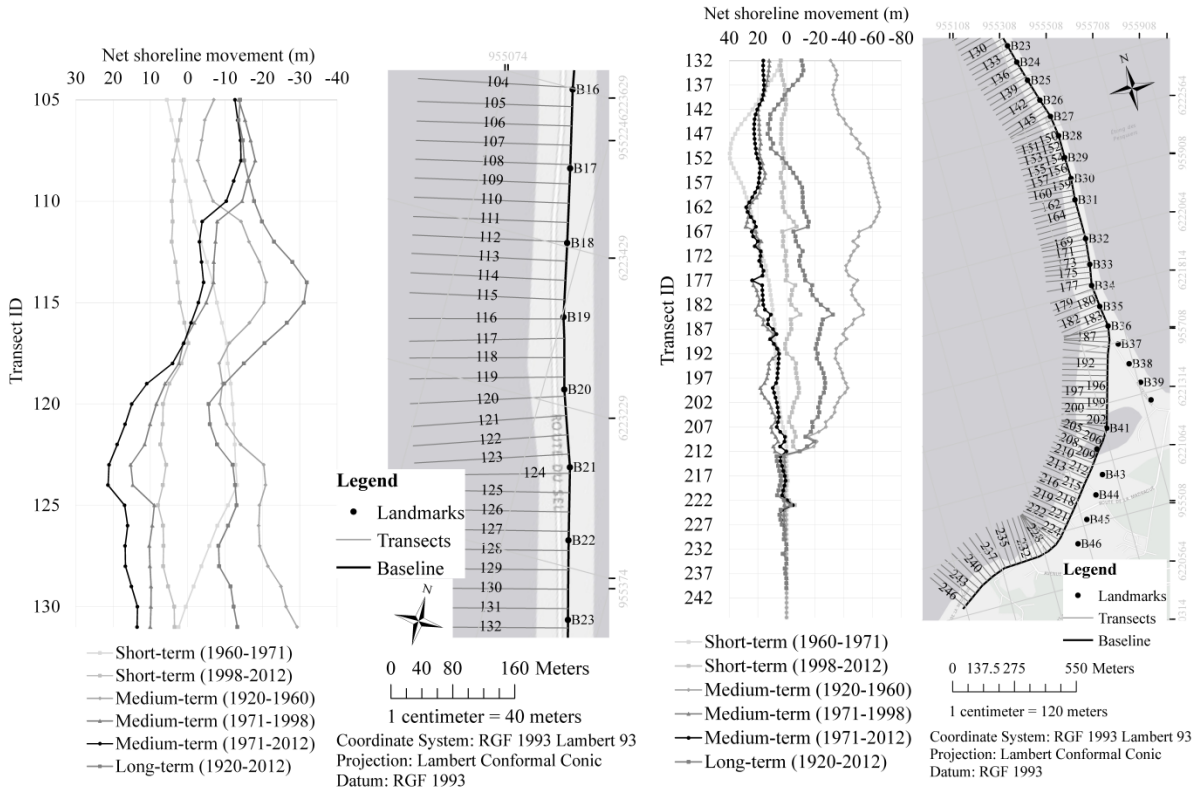

Fig. 6. Short, medium, and long term net shoreline movement along transects in the sectors 3 (left) and 4 (right) of the Western tombolo of Giens.

3.1.4. Sector 4

The number of transects of sector 4 are 115. Sector 4 consists of transects number 132 to 246. The South of sector 4 transects have numbers 224 to 246 (landmark B46 to southern end of the shoreline), and is stable (Fig. 6). The North of sector 4 from transects number 126 to 224 presents the greatest amount of erosion (about -65 m of NSM method) at transect number 162 in the medium term period of 1920-1960 (Fig. 6). It also registered the highest amounts of accretion (about 40 m of NSM method) at transect number 151 regarding short-term approach of 1960-1971 (Fig. 6).

3.2. Annual Shoreline Change Rates

Similarly, the results are exposed for each sector:

3.2.1. Sector 1

Only 9% of transects are erosional and 30% are accretional in the long term (Table 4). The average long term rate of change for all erosional transects in the sector 1 is -0.15 ± 0.12 m/yr by using WLR method (Table 4). Sector 1 is accreting at an average long-term rate of 0.04 ± 0.05 m/yr by LRR method (Table 4).

Fig. 7 summarizes the rate-of-change for each studied period. The maximum long-term erosion rate (-0.22 ± 0.16 m/yr) was found at transect number 47 (near landmark B02) by using WLR method (Fig. 7). The maximum long-term accretion rate (0.14 ± 0.19 m/yr) was found at transect number 38 (near landmark B01) by using EPR method. Along the sector 1 of coastline, the long-term (1920-2012) rates have similar trends with the short-term (1920-1960) ones, by using EPR method, or the other short-term (1971-1998) ones by using WLR method (Fig. 7). About 32% of transects are erosional in the short-term (1998-2012), and 23% are accretional from the long-term rate (1920-2012) (Table 4). The maximum short-term erosion rate (-0.98 ± 0.54 m/yr) was found at transect number 47 (near landmark B02) (Fig. 7). Maximum accretion rates were found at transect number 53 (about 0.93 ± 1.82 m/yr of the EPR method) for period of 1960-1971 (Fig. 7). In sector 1, the average medium-term rate (1971-2012) (-0.40 ± 0.15 m/yr in WLR method) indicates more erosion than the average long-term rate (1920-2012) (-0.15 ± 0.12 m/yr in WLR method) (Fig. 7).

Table 4

Shoreline change trends for sector 1 (North Zone) of the Western tombolo of Giens (negative and positive values indicate erosion and accretion, respectively).

Period		Short-term		Medium-term			Long-term
		1960-1971	1998-2012	1920-1960	1971-1998	1971-2012	
NTE		4	17	0	18	17	5
NTA		17	2	21	3	4	16
BE (m)		75	400	0	425	400	100
BA (m)		400	25	500	50	75	375
Rate BE (%)		8	32	0	34	32	9
Rate BA (%)		32	4	40	6	8	30
Minimal RE (m/yr)	E	-0.01	-0.05	0.00	-0.04	-0.06	-0.01
	L	0.00	-0.03	0.00	-0.02	-0.02	-0.01
	W	0.00	-0.02	0.00	-0.02	-0.07	-0.01
Average RE (m/yr)	E	-0.01	-0.38	0.00	-0.29	-0.33	-0.02
	L	0.00	-0.43	0.00	-0.26	-0.23	-0.02
	W	0.00	-0.63	0.00	-0.26	-0.40	-0.15
Maximal RE (m/yr)	E	-0.01	-0.62	0.00	-0.59	-0.47	-0.03
	L	0.00	-0.63	0.00	-0.46	-0.33	-0.06
	W	0.00	-0.98	0.00	-0.47	-0.58	-0.22
Minimal RA (m/yr)	E	0.13	0.08	0.01	0.05	0.00	0.01
	L	0.20	0.00	0.15	0.03	0.00	0.01
	W	0.20	0.03	0.15	0.03	0.01	0.01
Average RA (m/yr)	E	0.56	0.08	0.23	0.05	0.00	0.06
	L	0.51	0.00	0.28	0.03	0.00	0.04
	W	0.51	0.05	0.28	0.03	0.01	0.01
Maximal RA (m/yr)	E	0.93	0.08	0.36	0.05	0.00	0.14
	L	0.81	0.00	0.38	0.03	0.00	0.07
	W	0.81	0.07	0.38	0.03	0.01	0.01

NTE = number of transects erosion, NTA = number of transects accretion, BE = Beach erosion, BA = Beach accretion, E =EPR, L = LRR, W =WLR, RE = rate of erosion, RA = rate of accretion, km = kilometer, m/yr = meter per year.

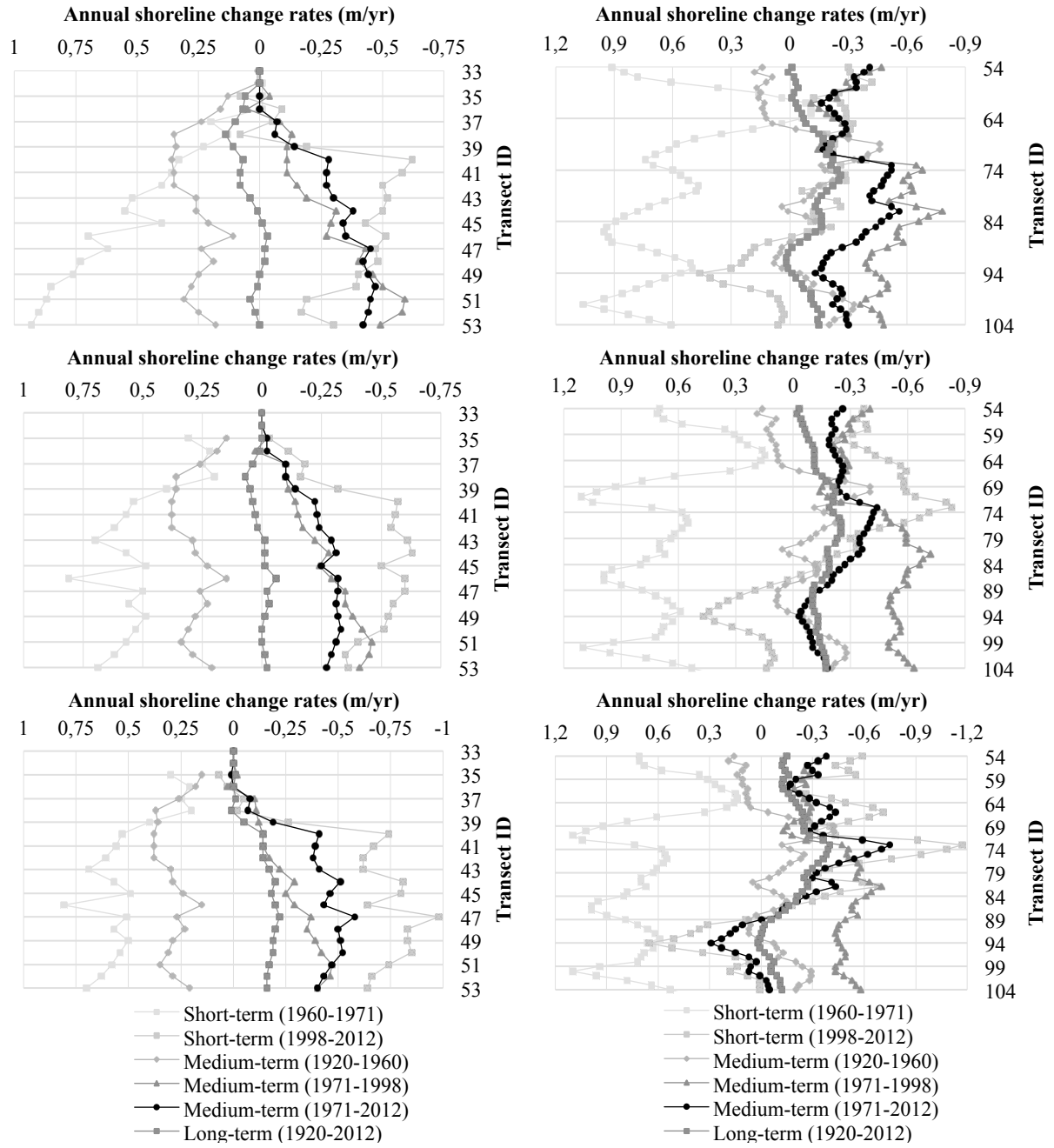

Fig. 7. Short, medium, and long term annual shoreline change rates in the sectors 1 (left) and 2 (right) of the Western tombolo of Giens using EPR (upper), LRR (middle), and WLR (lower) method.

3.2.2. Sector 2

This sector is highly erosional because of its exposure to the strong waves, winds and rip currents of the western and south-western regimes in winter. At the sector 2, majority of shorelines were eroded. Sector 2 is the most erosional sector of the Western tombolo of Giens (Table 5 and Fig. 7). The middle of sector 2 from transects number 65 to 88 are erosional in the long and short terms except one period of 1960-1971 (Fig. 7).

Erosion is the general long-term trend of the sector 2 (Fig. 7). 90% of transects are erosional in the long term. Sector 2 has the lowest rate of accreting beach (0 percent) of the four sectors in the period of 1971-1998 (Table 5).

Table 5

Shoreline change trends for sector 2 (North-central Zone) of the Western tombolo of Giens.

Period		Short-term	Medium-term				Long-term
		1960-1971	1998-2012	1920-1960	1971-1998	1971-2012	
NTE		4	34	32	51	51	46
NTA		47	17	19	0	0	5
BE (m)		75	825	775	1250	1250	1125
BA (m)		1150	400	450	0	-25	100
Rate BE (%)		8	67	63	100	100	90
Rate BA (%)		92	33	37	0	0	10
Minimal RE (m/yr)	E	-0.06	-0.01	-0.03	-0.11	-0.13	-0.01
	L	0.00	-0.04	-0.03	-0.14	-0.03	-0.02
	W	0.00	-0.09	-0.04	-0.13	-0.03	-0.01
Average RE (m/yr)	E	-0.09	-0.23	-0.20	-0.43	-0.32	-0.12
	L	0.00	-0.43	-0.17	-0.45	-0.22	-0.15
	W	0.00	-0.49	-0.19	-0.42	-0.32	-0.19
Maximal RE (m/yr)	E	-0.11	-0.42	-0.46	-0.78	-0.56	-0.26
	L	0.00	-0.83	-0.40	-0.72	-0.44	-0.25
	W	0.00	-1.17	-0.42	-0.70	-0.75	-0.40
Minimal RA (m/yr)	E	0.04	0.03	0.01	0.00	0.00	0.01
	L	0.15	0.03	0.02	0.00	0.00	0.00
	W	0.14	0.01	0.02	0.00	0.01	0.01
Average RA (m/yr)	E	0.65	0.18	0.10	0.00	0.00	0.01
	L	0.66	0.23	0.09	0.00	0.00	0.00
	W	0.66	0.24	0.08	0.00	0.13	0.01
Maximal RA (m/yr)	E	1.06	0.46	0.18	0.00	0.00	0.02
	L	1.11	0.47	0.19	0.00	0.00	0.00
	W	1.10	0.65	0.19	0.00	0.29	0.02

The average long-term erosion rate (1920-2012) is -0.19 ± 0.08 m/yr by using WLR method (Table 5). The maximum long-term erosion rate (-0.4 ± 0.16 m/yr) was calculated at transect number 73 (near landmark B08). Other areas also have significant long-term erosion rates (Fig. 7).

Approximately 100% of the short-term rates (1971-1998) are erosional, the highest percentage for the four sectors (Fig. 7). The medium and short term erosion rates (1971-1998 and 1998-2012) in sector 2 are the most erosional rates of the four sectors. The maximum short-term erosion rate (-1.17 ± 0.5 m/yr) was calculated at transect number 73 (near landmarks B08). Accretion rates have increased after the beach nourishment in short term period of 1960-1971 (Fig. 7). The average short-term accretion rate (0.66 ± 1.9 m/yr) was estimated by using LRR method for the period of 1960-1971.

3.2.3. Sector 3

Sector 3 is slightly erosional in the long term and accretional in the short term (1998-2012) (Fig. 8). The average long-term rate in sector 3 is erosional at -0.18 ± 0.07 m/yr by using LRR method (Table 6). Approximately 100% of transects are erosional in the long term (Table 6).

The maximum long-term erosion rate (-0.35 ± 0.16 m/yr) was estimated at transect number 114 (near landmark B19) (Table 6). The maximum long-term accretion rate (0.17 ± 0.14 m/yr) was found at transect number 127 (near landmark B22).

In opposition to long-term analysis, the short-term approach suggests a stable or accreting beach. We observed that short-term period of 1998-2012 in sector 3 indicates a trend of accretion (96% of

transects are accretional in Fig. 8). The average of short-term rates (1998-2012) is accretional at 0.44 ± 0.35 m/yr in the WLR method (Table 6). The maximum short-term accretion rate (0.76 ± 0.78 m/yr) was estimated at transect number 120 (near landmark B20).

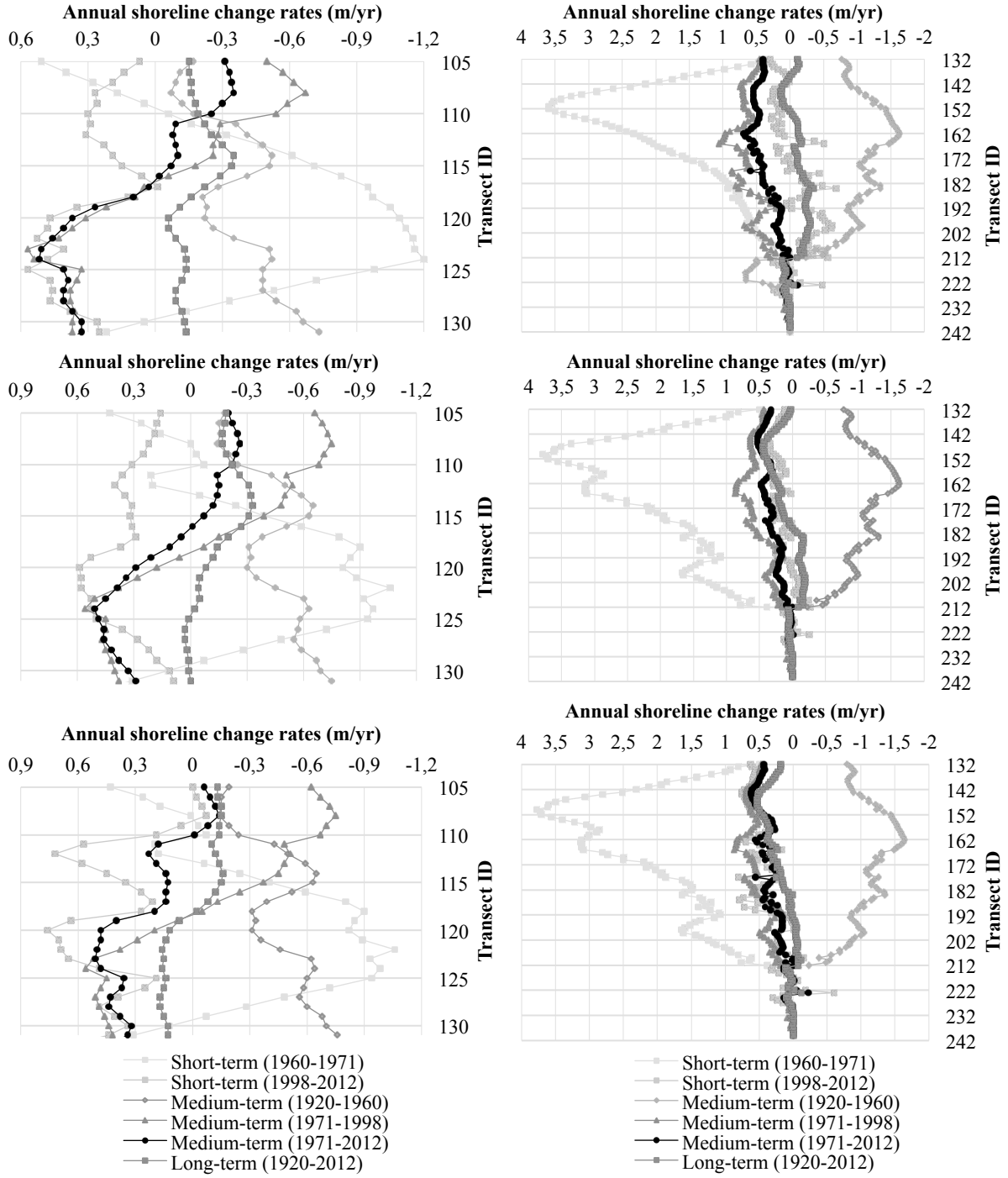

Fig. 8. Short, medium, and long term annual shoreline change rates in the sectors 3 (left) and 4 (right) of the Western tombolo of Giens using EPR (upper), LRR (middle), and WLR (lower) method.

Table 6

Shoreline change trends for sector 3 (Central Zone) of the Western tombolo of Giens.

		Short-term		Medium-term			
Period		1960-1971	1998-2012	1920-1960	1971-1998	1971-2012	Long-term
NTE		20	1	27	12	12	27
NTA		7	26	0	15	15	0
BE (m)		475	0	650	275	275	650
BA (m)		150	625	0	350	350	0
Rate BE (%)		74	4	100	44	44	100
Rate BA (%)		26	96	0	56	56	0
Minimal RE (m/yr)	E	-0.06	-0.01	-0.07	-0.06	-0.02	-0.06
	L	-0.03	0.00	-0.14	-0.07	-0.01	-0.02
	W	-0.03	-0.02	-0.14	-0.05	-0.01	-0.02
Average RE (m/yr)	E	-0.73	-0.01	-0.37	-0.40	-0.19	-0.17
	L	-0.58	0.00	-0.45	-0.51	-0.17	-0.18
	W	-0.59	-0.05	-0.45	-0.49	-0.08	-0.12
Maximal RE (m/yr)	E	-1.20	-0.01	-0.73	-0.67	-0.35	-0.35
	L	-1.06	0.00	-0.75	-0.75	-0.26	-0.33
	W	-1.06	-0.07	-0.76	-0.75	-0.14	-0.16
Minimal RA (m/yr)	E	0.05	0.06	0.00	0.05	0.03	0.00
	L	0.12	0.09	0.00	0.06	0.05	0.01
	W	0.01	0.06	0.00	0.08	0.13	0.07
Average RA (m/yr)	E	0.24	0.31	0.00	0.34	0.35	0.00
	L	0.24	0.34	0.00	0.38	0.35	0.02
	W	0.21	0.44	0.00	0.41	0.33	0.14
Maximal RA (m/yr)	E	0.51	0.57	0.00	0.57	0.52	0.00
	L	0.43	0.59	0.00	0.56	0.51	0.03
	W	0.43	0.76	0.00	0.56	0.51	0.17

3.2.4. Sector 4

The sector 4 presents trends of accretion in contrast to sector 2, except the short-term period of 1920-1960 (Fig. 8).

For the long-term period between 1920 and 2012, 58% of transects are erosional in the long-term approach (Table 7). The average long-term shoreline erosions were approximately stable at -0.17 ± 0.16 and -0.14 ± 0.21 m/yr for EPR and LRR method, respectively (Table 7). The maximum long-term erosion rate (-0.35 ± 0.16 m/yr) was found at transect number 184 (near landmark B36) (Table 7). This sector is accretional at 37% (long-term) and 46% (short-term period of 1998-2012) of transects, suggesting a general trend of erosion (Table 7). The sector 4 experienced accretions at average long term rates of 0.18 ± 0.25 and 0.22 ± 0.18 m/yr by using LRR and WLR method, respectively (Table 7). The sector 4 showed the highest accretion rate about 0.53 ± 0.18 m/yr at transect number 147 (near landmark B36) by using the WLR method (Table 7). Along the sector 4, long-term rates have trends similar to short-term rates except periods of 1920-1960 and 1960-1971 (Fig. 8). The short-term rates of 1920-1960 are opposite to the ones of 1960-1971 (Fig. 8).

Table 7

Shoreline change trends for sector 4 (South Zone) of the Western tombolo of Giens.

Period		Short-term		Medium-term			Long-term
		1960-1971	1998-2012	1920-1960	1971-1998	1971-2012	
NTE		9	43	81	0	2	67
NTA		83	53	24	109	107	42
BE (m)		200	1050	2000	-25	25	1650
BA (m)		2050	1300	575	2700	2650	1025
Rate BE (%)		8	37	70	0	2	58
Rate BA (%)		72	46	21	95	93	37
Minimal RE (m/yr)	E	-0.01	-0.01	-0.24	0.00	-0.01	-0.02

	L	0.00	-0.01	-0.22	0.00	-0.01	-0.04
	W	0.00	-0.01	-0.23	0.00	-0.01	-0.02
Average RE (m/yr)	E	-0.01	-0.32	-1.08	0.00	-0.06	-0.17
	L	0.00	-0.11	-1.06	0.00	-0.01	-0.14
	W	0.00	-0.14	-1.09	0.00	-0.06	-0.05
Maximal RE (m/yr)	E	-0.01	-0.69	-1.63	0.00	-0.11	-0.35
	L	0.00	-0.27	-1.62	0.00	-0.01	-0.19
	W	0.00	-0.60	-1.64	0.00	-0.22	-0.12
Minimal RA (m/yr)	E	0.01	0.02	0.01	0.03	0.02	0.01
	L	0.39	0.01	0.00	0.03	0.01	0.01
	W	0.38	0.01	0.00	0.03	0.01	0.01
Average RA (m/yr)	E	1.50	0.16	0.31	0.49	0.32	0.08
	L	2.01	0.18	0.00	0.41	0.26	0.18
	W	1.99	0.41	0.00	0.42	0.30	0.22
Maximal RA (m/yr)	E	3.60	0.31	0.67	1.06	0.69	0.14
	L	3.79	0.38	0.00	0.87	0.53	0.45
	W	3.78	0.81	0.00	0.87	0.62	0.53

4. Discussion

4.1. Distribution of Coefficient of Determination (R^2)

Fig. 9A represents the distribution of the values of the coefficient of determination along the Western tombolo.

These coefficients are pretty good in two areas: from the southern part of sector 1 to sector 2 and the northern part of sector 4. Majority of coefficient of determination vary from 0.25 to 0.75 (Fig. 9A). For the medium term approach (1971-2012), the coefficients of determination are greater than 0.5 between transects number 40 and 80 in the sector 2 and between transects number 140 and 180 in the northern part of sector 4.

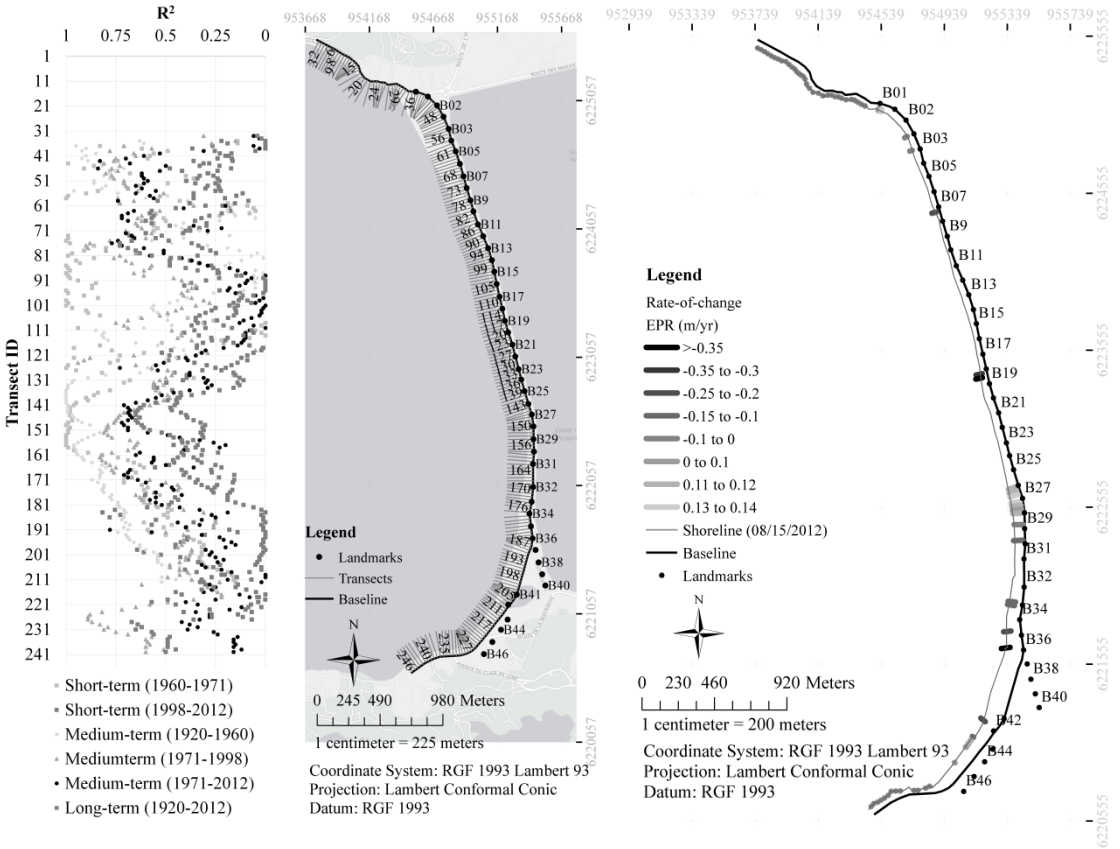

Fig. 9. (A) Distribution of coefficients of determination for WLR method in case of the Western tombolo. (B) Long-term (1920-2012) annual shoreline change rates, entire Western tombolo of Giens by using End Point Rate.

For the sector 3 and the southern part of sector 4, the coefficients of determination are not good. They are mainly distributed in the range of 0 to 0.5 (Fig. 9A). Between transects number 105 and 120, the coefficients of determination are smaller than 0.25 in the medium-term period (1971-2012). Transects number 190 to 230 also have more coefficients of determination in the range of 0.25 to 0.5.

4.2. Erosional and Accretional Trends

Fig. 9B summarizes the rates of change for long-term period by using the EPR method. The north zone (sectors 1 and 2) presents trends of erosion in contrast to the south zone (sectors 3 and 4). This evolution is closely comparable to the trends from the literature (Courtaud 2000; SOGREAH 1988b). The maximum long-term erosion rate (-0.35 ± 0.16 m/yr) was found at transect number 114 (near landmark B18 and B19, Fig. 9B). The average annual rate of shoreline retreat vary from -0.01 ± 1.82 to -0.63 ± 0.27 m/yr in the northern part. The Western tombolo showed the highest accretion rate about 0.14 ± 0.16 m/yr at transect number 147 (near landmark B26) (Fig. 9B). The average annual rate of shoreline accretion is estimated between 0.02 ± 0.14 and 2.01 ± 5.10 m/yr in the central and southern part of the Western tombolo.

4.3. Trends of Shoreline Movement

This study aims to forecast shoreline movements. A linear regression with a slope of an average annual rate-of-change was used. The extrapolations to ten, twenty, fifty, and a hundred years of the shoreline are made from the average rate of shoreline changes for the period from 1971 to 2012.

The average rate of shoreline erosion is between -0.22 ± 0.09 and -0.40 ± 0.15 m/yr for the sectors 1 and 2 and average rate of shoreline accretion is between 0.26 ± 0.17 and 0.35 ± 0.18 m/yr for the sectors 3 and 4, respectively.

Table 8 shows the trends of shoreline movement for the Western tombolo in ten, twenty, fifty and a hundred years. The coastline in short-term (2022) was predicted to recede at least –2.2 ± 0.9 m in the sectors 1 and 2. Similarly, the average shoreline recession in year 2032 was predicted to be at least -4.4 ± 1.8 m. In long-term (2112) along sectors 1 and 2, coastline would retreat at a distance of 22 m (Table 8).

Table 8

Prediction of future shoreline movement for the Western tombolo.

Sector	Average rates from 1971 to 2012 (m/yr)		Trends of shoreline movement (m)			
			10	20	50	100
					(years)	
1	EPR	-0.33	-3.3	-6.5	-16.3	-32.6
	LRR	-0.23	-2.3	-4.6	-11.6	-23.1
	WLR	-0.40	-4.0	-7.9	-19.8	-39.6
2	EPR	-0.32	-3.2	-6.3	-15.8	-31.5
	LRR	-0.22	-2.2	-4.4	-11.1	-22.1
	WLR	-0.32	-3.2	-6.4	-16.1	-32.2
3	EPR	0.35	3.5	7.1	17.7	35.5
	LRR	0.35	3.5	6.9	17.3	34.5
	WLR	0.33	3.3	6.5	16.3	32.6
4	EPR	0.32	3.2	6.3	15.8	31.6
	LRR	0.26	2.6	5.2	12.9	25.9
	WLR	0.30	3.0	6.0	15.1	30.2

Negative and positive values indicate erosion and accretion, respectively.

4.4. Shoreline Change and Some Factors of Coastal Erosion

4.4.1. Waves and Shoreline Changes

The statistics of wave data available from 1999 to 2012 (14 years) at the buoy Porquerolles - 08301 helps to define the annual wave regime (annual condition). The nearshore significant wave heights were extracted from the simulation in Mike 21 (Lacroix et al. 2015b) for all transects in the annual condition (Fig. 10A). The strong waves are focused between transects number 50 and 104 in Fig. 10A.

The linear regressions among net shoreline movement/rates of change (y) and significant wave height (x) in m were found in Fig. 10B,C. There coefficients of determination are not bad (R^2 = 0.35). These dispersions show that the shoreline erosions are proportional to the significant wave height. A significant wave height change of 1 cm causes a variation of net shoreline movement of about -37.6 cm (Fig. 10B) and rates of changes variation of about -0.9 cm/yr (Fig. 10C).

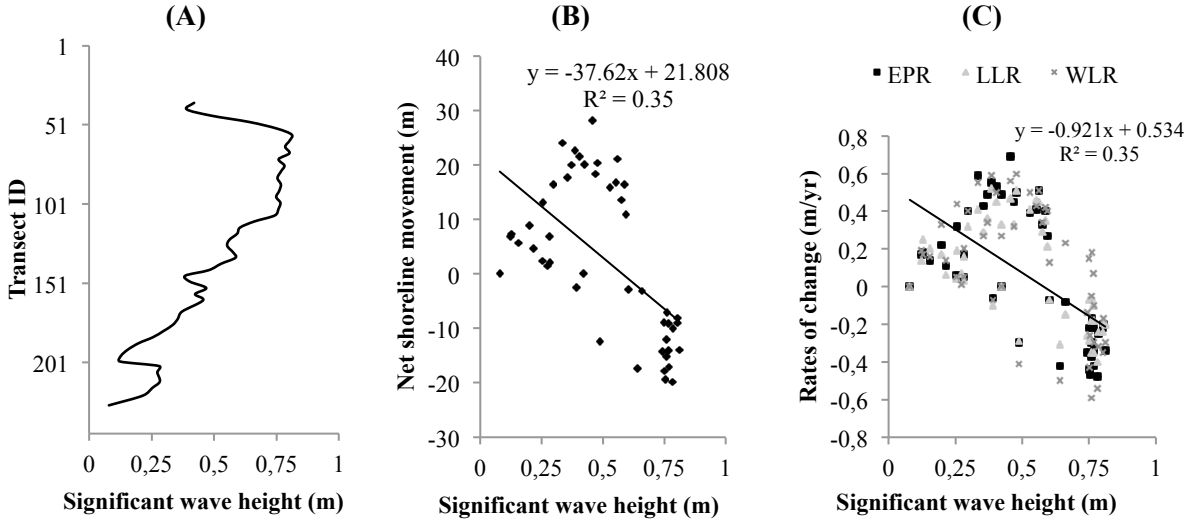

Fig. 10. (A) Nearshore significant wave height at the different transects in the Western tombolo. (B) Relation between net shoreline movement and nearshore significant wave height. (C) Relation between rates of change and nearshore significant wave height.

4.4.2. Sea Level Rise and Shoreline Retreats

According to the Ministry of Environment / SRETIE, the sea level rise may reach up to 8 mm/yr on the French coast (HYDRO M 1993). But, in the 20th century, it seemed to be between 1.8 mm/yr (Jarry 2009) and 2-3 mm/yr (HYDRO M 1993). Brunel (2010) has estimated the variation in the mean sea level due to global warming for the 21st century (LENOBLE 2010). Between 2010 and 2060, the variation in the mean sea level can reach + 35 cm (LENOBLE 2010). According to SOGREAH (1988b), the sea level rise is in the order of 1-2 mm/yr. The relative sea level trends of +1.29 ± 0.13 mm/yr for 1885-2013 and +3.62 ± 0.99 mm/yr for 1984-2013 have been calculated at Marseille station by Permanent Service of Mean Sea Level (PSMSL)

The annual data of MSL was taken from PSMSL for Toulon station from 1994 to 2013 with respect to Revised Local Reference (RLR - a reference vertical) (Fig. 11A). A linear regression of sea level in Toulon was tested. A linear regression was found and described by the equation $y = 3x + 722$, where: y is the water level in mm; x is year. This regression indicates a sea level rise in Toulon; this is quite consistent with the rising trend of sea level in general. However, its coefficient of determination is bad ($R^2 = 0.26$) (Fig. 11A). The sea level rise can reach 3 mm/yr based on the water level data for period of 1994-2013 (Fig. 11A).

The dispersion among net shoreline erosion (y) in m and sea level rise (x) in mm was estimated by using a linear regression as $y = -0.054x – 0.947$. This regression indicates that the net shoreline erosion is proportional to sea level rise. But its determination coefficient is very bad ($R^2 = 0.1$). With a sea level rise change of 1 mm, the net shoreline erosion variation is -0.054 m (Fig. 11B).

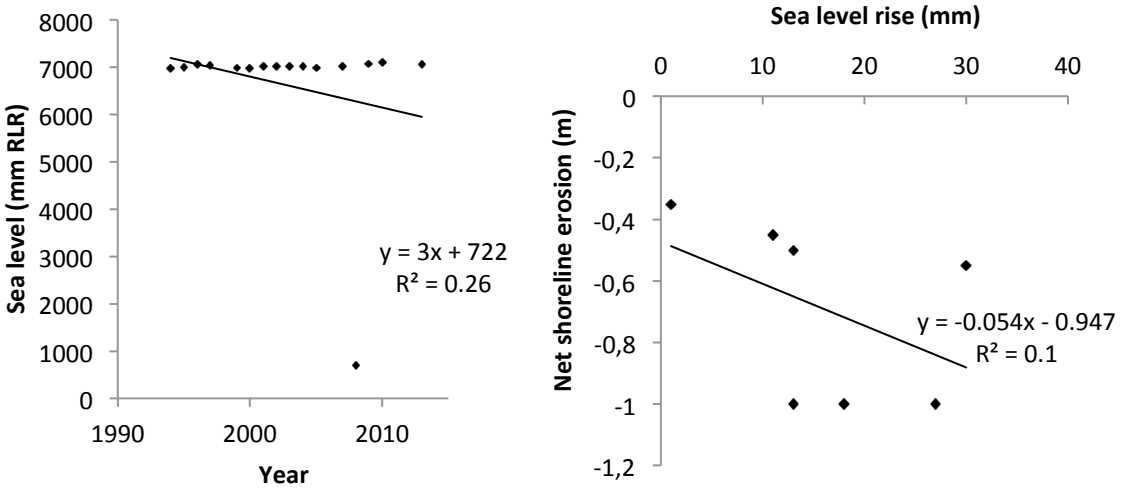

Fig. 11. (A) Yearly average annual sea level in mm RLR (referred to Revised Local Reference datum) at the station Toulon (source: PSMSL). (B) The interactive relationship between average sea level change and net shoreline erosion over the period from 1998 to 2010.

4.4.3. Beach slope and Shoreline Changes

The beach slope has an important role in mitigating or accelerating rip-currents. The Gulf of Giens presents a relatively low average beach slope (Courtaud 2000). However, ERAMM (2001) highlights strong gradients of the beach slope near the coast in some beach profiles. The very strong beach slope (approximately 10%) limits greatly sedimentary exchanges between the emerged and immersed parties in the beach profile (ERAMM 2001). During storms, sediments driven by rip currents out to sea cannot return to the coast by the waves of good weather because the beach slope is too strong (ERAMM 2001).

The beach slope is highest from transects number 50 to 100 (Fig. 12A). It is strong in the first 100 m of the profile limited by -2 m contours. Then, from the -2 m contours, it is very low on the rest of the profile (ERAMM 2001).

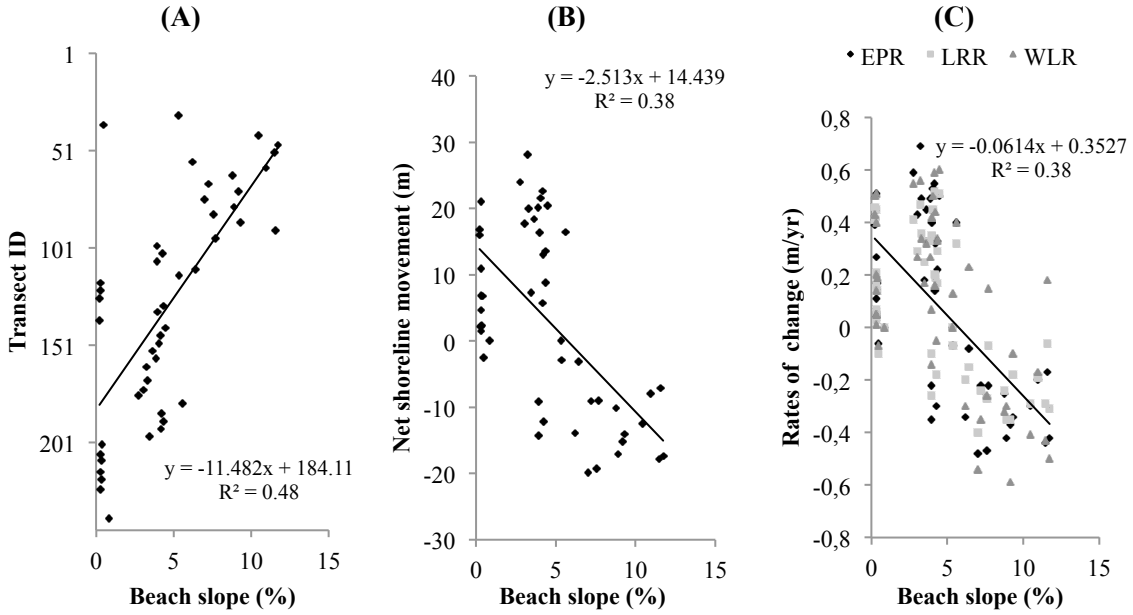

Fig. 12. (A) Beach slope of the first 100 m of the Almanarre beach profile (in %) at the different transects. (B) Relation between net shoreline movement and beach slope. (C) Relation between rates of change and beach slope.

We observe that net shoreline movement/rates of change and beach slope have a reasonable linear correlation, with $R^2 = 0.38$ (Fig. 12B,C). An equilibrium beach slope of the first 100 m of the beach profile can be estimated about 5%. ERAMM (2001) indicates an equilibrium beach slope of 3-5% in the nearshore.

4.4.4. Shoreline Orientation and Shoreline Changes

For the Western tombolo, the orientations of the coastline vary between 200° and 310° (Fig. 13A). On the northern part of the tombolo, the shoreline orientations are from 200° to 258°. The net transit is very sensitive to the shoreline orientation (Than 2015): a pivot 1° of the shoreline orientation can cause a significant change in the net transit of about 2 000 m^3/yr (cubic meters per year).

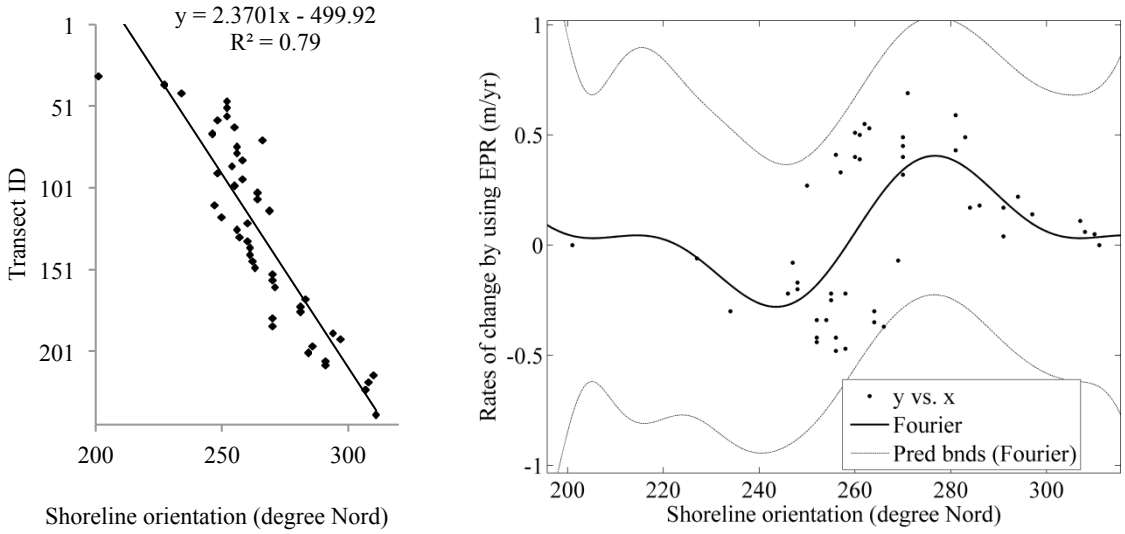

Fig. 13. (A) Shoreline orientation of the Almanarre beach (in degree Nord) at the different transects. (B) Relation between rates of change and shoreline orientation by using a Fourier two orders.

We observe that shoreline orientation seems to be proportional with transect number (transect ID) with a good correlation ($R^2 = 0.79$) in Fig. 13A. The dispersion of rates of change and shoreline orientation can be estimated by using two Fourier orders with a weak correlation ($R^2 = 0.34$) (Fig. 13B). An equilibrium orientation of the coastline is located approximately 262° (Fig. 13B).

5. Conclusion

We conclude that DSAS is effective to determine the zone of erosion and accretion and to estimate the overall change in historical shoreline position by using the extracted shorelines. An analysis of Net Shoreline Movement was undertaken. We suggest that DSAS is helpful for the management of the coastal area. We consider that the methodological approaches in this paper can be used for other coasts.

The annual historical shoreline change rates are simply quantifiable by DSAS. The rates-of-change were calculated along transects. Average erosion rates are estimated to be (-0.01 to -0.63) ± (0.27 to 1.82) m/yr for sectors 1 and 2. Average accretion rates is (0.02 to 2.01) ± (0.14 to 5.10) m/yr for the sector 3 and 4.

Individual rates along some transect in northern part of the Western tombolo reach as high as -1.17 ± 0.5 m/yr. The rates of change calculated are closely comparable with the trends noted in the literature (Courtaud 2000; SOGREAH 1988b).

The correlation coefficients are pretty good in the southern part of sector 1, sector 2, and northern part of sector 4. They are weak for the sector 3 and the southern part of sector 4.
The prediction of future shoreline movements was carried out by using an extrapolation of the average annual historical shoreline change rates. The coastline in short term (2022) was predicted to recede at least –2.2 ± 0.9 m in the sectors 1 and 2. Similarly, the average shoreline recession in year 2032 was predicted to be at least -4.4 ± 1.8 m. In long term (2112) along sectors 1 and 2, coastline would retreat at a distance of 22 m.
The strong waves focus between transects number 50 and 104. Shoreline erosions are proportional to the significant wave heights. A variation of significant wave height of 1 cm generates a variation of net shoreline erosion about -37.6 cm and rates of changes about -0.9 cm/yr.
We conclude that a rising trend of sea level during the period of 1994-2013 in Toulon harbor correlates to the general increasing trend of Mean Sea Level. The sea level rise can reach 3 mm/yr in the Western tombolo. The results show that the net shoreline erosion is proportional to sea level rise. With a sea level rise change of 1 mm, the shoreline retreat variation is -0.054 m.
The beach slope is highest from transects number 50 to 100. We observe that net shoreline movement/rates of change and beach slope have a reasonable linear correlation. An equilibrium beach slope of the first 100 m of the beach profile can be estimated about 5%.
On the northern part of the tombolo, the shoreline orientation is from 200° to 258°. We observe that shoreline orientation seems to be proportional with transect number with a good correlation. The dispersion of rates of change and shoreline orientation can be estimated by using a second order Fourier approximation. An equilibrium orientation of the coastline is located approximately 262°.
The shoreline change analysis in the Western tombolo helps to determine the key factors driving the shoreline change. Our work will also help to propose possible solutions to stabilize the shoreline. This subject will be the focus of a forthcoming paper by the authors.

List of acronyms

DSAS	Digital Shoreline Analysis System
NSM	Net Shoreline Movement
EPR	End Point Rate
WLR	Weighted Linear Regression
LRR	Linear Regression Rate
CEREGE	Centre de Recherche et d'Enseignement de Géosciences de l'Environnement
SHOM	Service Hydrographique et Océanographique de la Marine
IGN	Institut national de l'information géographique et forestière
IFN	Inventaire Forestier National
EOL	Etude et Observation du Littoral
PSMSL	Permanent Service for Mean Sea Level
REFMAR	Réseaux de rEFérence des observations MARégraphiques
EDF	Électricité de France
USGS	United States Geological Survey
MSL	Mean Sea Level
RLR	Revised Local Reference

List of symbols

E_s	seasonal error
E_t	tidal error
E_d	digitizing error
E_p	pixel error

E_r	rectification error
i	index of the shoreline
U_{ti}	total positional uncertainty for each shoreline i
T	period of analysis
R	rate-of-change in meters per year (m/yr)
D	net shoreline movement in meters
T_e	time period elapsed between the oldest and the most recent shoreline (years)
y	distance from baseline
m, m_w	slope
b, b_w	y-intercept (where the line crosses the y-axis)
R^2	Coefficient of Determination

Acknowledgements

We would like to thank the following organizations who have kindly provided data possible: CEREGE, SHOM, IGN, EOL, PSMSL and REFMAR. We also thank USGS for the DSAS tool for this paper.

References

Addo, K.A., Jayson-Quashigah, P.N., & Kufogbe, K.S. (2011). Quantitative analysis of shoreline change using medium resolution satellite imagery in Keta, Ghana. *Marine Science, 1*, 1-9

Anders, F.J., & Byrnes, M.R. (1991). Accuracy of shoreline change rates as determined from maps and aerial photographs. *Shore and Beach, 59*, 17–26

Blanc, J.J. (1960). Etude sédimentologique de la presqu l'île de Giens et de ses abords. In (pp. 35-52)

Blanc, J.J. (1974). Phénomènes d'érosions sous-marines à la Presqu'île de Giens (Var). *CR Acad. Sci. Paris, 278*, 1821-1823

Brunel, C. (2010). Évolution séculaire de l'avant côte de la méditerranée Française, impact de l'élévation du niveau de la mer et des tempêtes. In, *U.F.R des Sciences Géographiques et de l'Aménagement* (p. 470). Marseille: Université de Provence-Aix-Marseille I

Chand, P., & Acharya, P. (2010). Shoreline change and sea level rise along coast of Bhitarkanika wildlife sanctuary, Orissa: an analytical approach of remote sensing and statistical techniques. *International Journal of Geomatics and Geosciences, 1*, 436-455

Courtaud, J. (2000). Dynamiques geomorphologiques et risques littoraux cas du tombolo de giens (Var, France méridionale). In (p. 263): Université Aix-Marseille I

Crowell, M., Leatherman, S.P., & Buckley, M.K. (1991). Historical Shoreline Change: Error Analysis and Mapping Accuracy. *JOURNAL OF COASTAL RESEARCH, 7*, 839-852

Dang, V.T., & Pham, T.P.T. (2008). A shoreline analysis using DSAS in Nam Dinh coastal area. *International Journal of Geoinformatics, 4*, 37-42

ERAMM (2001). Etude sur la protection de la partie Nord du tombolo Ouest de Giens. In

Farnole, P., Bougis, J., Ritondale, M., & Barbarroux, M. (2002). Protection du littoral contre l'érosion marine: application au tombolo Ouest de Giens. In, *VIIèmes Journées Nationales Génie Civil- Génie Côtier* (pp. 513-522). Anglet, France: Editions Paralia

Faye, I., Giraudet, E., Gourmelon, F., & Henaff, A. (2011). Cartographie normalisée de l'évolution du trait de côte. *Mappemonde, 104*, 12

Fletcher, C.H., Romine, B.M., Genz, A.S., Barbee, M.M., Dyer, M., Anderson, T.R., Lim, S.C., Vitousek, S., Bochicchio, C., & Richmond, B.M. (2011). National assessment of shoreline change: Historical shoreline change in the Hawaiian Islands. In (p. 55)

Genz, A.S., Fletcher, C.H., Dunn, R.A., Frazer, L.N., & Rooney, J.J. (2007). The predictive accuracy of shoreline change rate methods and alongshore beach variation on Maui, Hawaii. *JOURNAL OF COASTAL RESEARCH*, 87-105

GEOMER (1996). Aménagement du littoral- Etude de faisabilité d'un port intérieur à l'embouchure du Gapeau: Etude courantologique et sédimentologique. In. Marseille

Himmelstoss, E.A. (2009). DSAS 4.0 Installation Instructions and User Guide. *in: Thieler, E.R., Himmelstoss, E.A., Zichichi, J.L., and Ergul, Ayhan. 2009 Digital Shoreline Analysis System (DSAS) version 4.0 — An ArcGIS*

*extension for calculating shoreline change: U.S. Geological Survey Open-File Report 2008-1278. *updated for version 4.3*. (p. 79)
HYDRO M (1993). Etude d'impact sur l'environnement du projet de protection du tombolo ouest de la presqu'ile de Giens. In
IARE (1996). Le Tombolo Occidental de Giens - Synthèse des connaissances- Analyse globale et scenarios d'aménagement et de gestion. In
IFEN (2007). Analyse statistique et cartographique de l'érosion marine. In (p. 36). Orléans
Jamont, M.F. (2014). Etude des aléas naturels sur le «Sud Vendée et marais Poitevin» - Rapport de phase 2 - Caractérisation des aléas de référence. In (pp. 67-67). Vendée
Jarry, N. (2009). Etudes expérimentales et numériques de la propagation des vagues au-dessus de bathymétries complexes en milieu côtier. In (p. 339): Université du Sud Toulon Var
Jeudy De Grissac, A. (1975). Sédimentologie dynamique des rades d'Hyères et de Giens (Var). Problèmes d'Aménagements. In (p. 86 + annexes). Marseille: Université d'Aix-Marseille II
Lacroix, Y., Than, V.V., Leandri, D., & Liardet, P. (2015a). Analysis of a Coupled Hydro-Sedimentological Numerical Model for the Tombolo of GIENS. *International Journal of Environmental, Ecological, Geological and Geophysical Engineering, 9*, 117 - 124
Lacroix, Y., Than, V.V., Leandri, D., & Liardet, P. (2015b). Analysis of Some Solutions to Protect the Tombolo of GIENS. *International Journal of Environmental, Ecological, Geological and Geophysical Engineering, 9*, 108 - 116
LENOBLE, A. (2010). Etude pour la protection de la plage du Ceinturon et du secteur Sud du port Saint-Pierre – Phase 1 : Synthèse des connaissances - Rapport. In
Luhar, M., Coutu, S., Infantes, E., Fox, S., & Nepf, H. (2010). Wave-induced velocities inside a model seagrass bed. *Journal of Geophysical Research: Oceans (1978–2012), 115*
Moore, L.J. (2000). Shoreline mapping techniques. *JOURNAL OF COASTAL RESEARCH, 16*, 111-124
Oyedotun, T.D.T. (2014). Shoreline Geometry: DSAS as a Tool for Historical Trend Analysis. *Geomorphological Techniques, Chap. 3, Sec. 2.2 (2014)*, 12
Prukpitikul, S., Buakaew, V., Keshdet, W., Kongprom, A., & Kaewpoo, N. (2012). Shoreline Change Prediction Model for Coastal Zone Management in Thailand. *Journal of Shipping and Ocean Engineering, 2*, 238-243
Robichaud, A., Simard, I., & Chelbi, M. (2012). Erosion et infrastructures à risque à Sainte-Marie-Saint-Raphaël, Péninsule acadienne, Nouveau-Brunswick. In (p. 39)
Romine, B.M., & Fletcher, C.H. (2012). A summary of historical shoreline changes on beaches of Kauai, Oahu, and Maui, Hawaii. *JOURNAL OF COASTAL RESEARCH, 29*, 605-614
Salghuna, N.N., & Bharathvaj, S.A. (2015). Shoreline Change Analysis for Northern Part of the Coromandel Coast. *Aquatic Procedia, 4*, 317-324
Serantoni, P., & Lizaud, O. (2000-2010). Suivi de l évolution des plages de la commune Hyères-les-palmiers. In
SOGREAH (1988a). Défense du littoral oriental du golfe de Giens. In (p. 50 + annexes)
SOGREAH (1988b). Protection du tombolo Ouest. In
Than, V.V. (2015). Modélisation d'érosion côtière : application à la partie Ouest du tombolo de Giens. In, *LATP* (p. 400). Marseille: Aix Marseille Université
Thieler, E.R., & Danforth, W.W. (1994). Historical Shoreline Mapping (I): Improving Techniques and Reducing Positioning Errors. *JOURNAL OF COASTAL RESEARCH, 10*, 549-563
Thieler, E.R., Himmelstoss, E.A., & Miller, T. (2005). Digital Shoreline Analysis System (DSAS) version 3.0: An ArcGIS extension for calculating shoreline change. In, *Extension for ArcGIS*
Thieler, E.R., Martin, D., & Ergul, A. (2003). The Digital Shoreline Analysis System, version 2.0: Shoreline change measurement software extension for ArcView. In, *Extension for ArcGIS*